Bioorganic & Medicinal Chemistry 19 (2011) 1268–1276

Contents lists available at ScienceDirect

Bioorganic & Medicinal Chemistry

journal homepage: www.elsevier.com/locate/bmc

Amyrin esters induce cell death by apoptosis in HL-60 leukemia cells

Francisco W. A. Barros [a], Paulo N. Bandeira [b], Daisy J. B. Lima [a], Assuero S. Meira [a], Silvana S. de Farias [b], Maria Rose J. R. Albuquerque [b], Hélcio S. dos Santos [b], Telma L. G. Lemos [c], Manoel Odorico de Morais [a], Letícia Veras Costa-Lotufo [a], Claudia do Ó Pessoa [a,*]

[a] Departament of Physiology and Pharmacology, Federal University of Ceará, Fortaleza, Ceará 60430-270, Brazil
[b] Laboratory of Organic Chemistry, State University Vale do Acarau, Sobral, Ceará 62040-370, Brazil
[c] Departament of Organic and Inorganic Chemistry, Ceara Federal University, Fortaleza, Ceará 60431-970, Brazil

ARTICLE INFO

Article history:
Received 13 September 2010
Revised 29 November 2010
Accepted 4 December 2010
Available online 9 December 2010

Keywords:
Protium heptaphyllum
Derivatives of α,β-amyrin
Cytotoxic activity
Apoptosis

ABSTRACT

Four derivatives of an α,β-amyrin mixture were synthesized by acylation with appropriate anhydrides. The structures of the compounds were confirmed by means of IR and ^{1}H and ^{13}C NMR. The compounds were screened for cytotoxic activity using four human tumor cell lines (HL-60, MDAMB-435, SF-295 and HCT-8) and normal peripheral blood mononuclear cells (PBMC). 3-*O*-Carboxymaleinate of α,β-amyrin (**3a**/**3b**) were found to be the only active compounds of the series (high cytotoxicity), showing IC_{50} values ranging from 1.8 to 3 μM. In PBMC, **3a**/**3b** were not toxic, suggesting selectivity for tumor cells. To better understand the mechanism of action involved in the cytotoxicity of **3a**/**3b**, HL-60 cells treated with **3a**/**3b** were examined for morphological changes, DNA fragmentation, cell cycle perturbation, externalization of phosphatidylserine and activation of caspases 3/7, with doxorubicin serving as the positive control. The results indicate that the cytotoxicity of **3a**/**3b** involves the induction of cell death by apoptosis.

1. Introduction

Triterpenoids are compounds that have attracted much interest because of their structural diversity and the discovery of a broad spectrum of pharmacological activities, such as anti-inflammatory, gastroprotective, antimicrobial, antinociceptive, antioxidant, analgesic, anticancinorgenic, cytotoxic and antidepressive effects.[1–11] In the last ten years, a large number of synthetic derivatives of natural triterpenoids have contributed significantly to the pharmacological study of these compounds.[12,13]

In this respect, the pentacyclic triterpenes α,β-amyrin, naturally occurring in many species, especially in the resin of species of *Protium*, possess anti-inflammatory, gastoprotective, antinociceptive, antidepressant, antiplatelet and analgesic activities.[6,9,10,14] Studies on *Protium heptaphyllum* resin showed that it also has anti-inflammatory, gastroprotective, anti-allergic and antinociceptive properties. These and other biological effects have been attributed to the presence of pentacyclic triterpenes, especially α,β-amyrin.[14,15]

The triterpenoid mixture known as α,β-amyrin has a basic skeleton of the ursan and olean type, respectively. Whose main difference is in the position of the methyl group in the E ring located at C-20. Its structural similarity with steroidal drugs may explain its broad pharmacological activity.[14] Although the pentacyclic triterpenes α,β-amyrin have weak anticancer activity, many other triterpene compounds, in contrast, have shown strong cytotoxic effects against various human tumor cells.[11] Investigations of the cytotoxic effects of these compounds have been conducted, and studies show that this effect is related to the induction of apoptosis.[11,16,17]

Taking into account that small changes in a molecule can significantly alter its pharmacological activity,[18] the objective of this work was the synthesis of new derivatives of α,β-amyrin, specifically esters modified at C-3 of the A ring, and evaluation of their cytotoxic activities against four human cancer cell lines and mononuclear cells from human peripheral blood (PBMC), used as a model of normal cells

2. Results and discussion

2.1. Chemistry

In order, to obtain derivatives **1a**/**1b**, **2a**/**2b**, **3a**/**3b** and **4a**/**4b**, the α,β-amyrin (**a**/**b**) mixture was isolated from the resin of *Protium heptaphyllum*.[19] The synthesis of the derivatives is outlined in Figure 1.

2.1.1. Isolation and structural elucidation of the mixture of α- and β-amyrin (a/b)

The mixture of triterpenoid α,β-amyrin (**a**/**b**) was isolated from the resin of *Protium* heptaphyllum[19] and analyzed by ^{1}H NMR,

* Corresponding author at present address: Departmento de Fisiologia e Farmacologia, Universidade Federal do Ceará, Rua Cel. Nunes de Melo, 1127, PO Box 3157, 60430-270 Fortaleza, Ceará, Brazil. Tel.: +55 85 3366 8341; fax: +55 85 3366 8333.
E-mail address: cpessoa@ufc.br (Claudia do Ó Pessoa).

0968-0896/$ - see front matter © 2010 Elsevier Ltd. All rights reserved.
doi:10.1016/j.bmc.2010.12.016

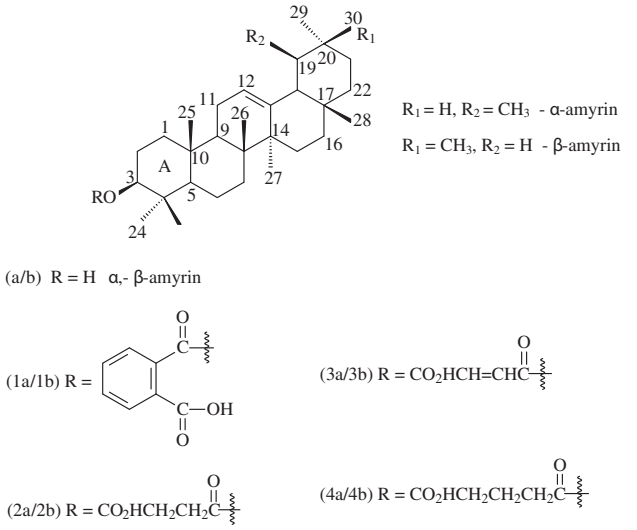

Figure 1. Derivatives of α,β-amyrin: (**1a**/**1b**) phthalic anhydride, py, reflux (50 °C), ethyl ether, 8 h. (**2a**/**2b**) succinic anhydride, DMAP, reflux (50 °C), CH_2Cl_2, 8 h. (**3a**/**3b**) maleic anhydride, reflux (50 °C), CH_2Cl_2, 8 h. (**4a**/**4b**) glutaric anhydride, DMAP, reflux (50 °C), CH_2Cl_2, 8 h.

enabling the determination of a 2:1 ratio, respectively. The structure elucidation was based on spectral data (IR, ^{1}H NMR, ^{13}C NMR). The IR spectra showed mainly absorptions bands at 3307 cm^{-1} assigned to hydroxyl group (OH) and 1460–1383 cm^{-1} characterisitics of C=C. In the ^{1}H NMR spectra of **a**/**b**, δ 0.80–2.10 ppm (characteristic profile of the α,β-amyrin). H-3 appears as a double–doublet at δ = 3.22 ppm with ^3J = 10.4 and 5.0 Hz of the α-amyrin and as a double–doublet at δ = 3.23 with ^3J = 10.4 and 5.0 Hz of the β-amyrin. H-12 appears as a triplet at δ = 5.10 ppm with ^3J = 3.6 Hz of the α-amyrin and δ = 5.10 ppm with ^3J = 3.6 Hz of the β-amyrin. In the ^{13}C NMR, the signal for C-3 is at δ = 79.1 ppm, while C-12 appears at δ = 124.4 ppm of the α-amyrin and δ = 21.7 ppm of the β-amyrin and C-13 appears at δ = 139.6 ppm of the α-amyrin and δ = 145.2 ppm of the β-amyrin.

2.1.2. Structural elucidation of the α,β-amyrin derivatives

The IR spectra of the mixture **1a**/**1b** showed one absorption band at 1701 cm^{-1} assigned to (C=O) of esters, typical absorption band of (OH) of acids, and absorption bands between 1583 and 1404 cm^{-1} of (C=C) of the aromatic ring.

In the ^{1}H NMR spectra of **1a**/**1b**, δ 0.80–2.10 ppm (characteristic profile of the substrate), H-3 appears as a double–doublet at δ = 4.77 ppm with ^3J = 8.1 and 3.5 Hz and H-12 as a triplet at δ = 5.13 ppm of the α-amyrin derivative and δ = 5.19 ppm of the β-amyrin derivative with ^3J = 3.6 Hz. Signals for aromatic hydrogen were identified at δ 7.27–7.88. In the ^{13}C NMR, the signal for C-3 is at δ = 83.3 ppm, while C-12 appears at δ = 124.5 ppm of the α-amyrin derivative and δ = 121.9 ppm of the β-amyrin derivative, C-13 appears at δ = 139.8 ppm of the α-amyrin derivative and δ = 145.4 of the β-amyrin derivative. Signals for aromatic carbon are in the range of δ 129.1–133.4 ppm. The C=O carbon atoms appears at δ = 168.1 ppm for esters and δ = 172.1 for acids. MS (70 eV) *m*/*z* (%) 574 (37, M^+), 573.39 (100).

Analysis of the IR spectra of **2a**/**2b** allowed absorption bands for (C=O) of esters at 1715 cm^{-1} and for (C=O) of acids at 1731 cm^{-1}, one absorption band at 2925 cm^{-1} identified as the (OH) of acids and absorption bands between 1633 and 1376 cm^{-1} of (C=C), characteristic of alkenes.

In the ^{1}H NMR spectra of **2a**/**2b**, δ 0.80–2.10 ppm (characteristic profile of the substrate), H-3 appears as a double–doublet at δ = 4.54 ppm and H-12 as a triplet at δ = 5.13 ppm of the α-amyrin derivative and δ = 5.21 ppm of the β-amyrin derivative. Signal for H-1′ is at δ = 2.69 ppm as doublet with ^3J = 5.65 Hz and H-2′ at δ = 2.64 ppm as dublet with ^3J = 5.85 Hz. In the ^{13}C NMR, the signal for C-3 is at δ = 81.8 ppm, while C-12 appears at δ = 124.5 ppm of the α-amyrin derivative and δ = 121.8 ppm of the β-amyrin derivative, C-13 appears at δ = 139.9 ppm of the α-amyrin derivative and δ = 145.4 ppm of the β-amyrin derivative. Signal for H-1′ is at δ = 2.69 ppm as dublet with ^3J = 5.65 Hz and H-2′ at δ = 2.64 ppm as dublet with ^3J = 5.85 Hz. The C=O carbon atoms appear at δ = 172.0 ppm for esters and δ = 168.1 ppm for acids. MS (70 eV) *m*/*z* (%) 526 (44, M^+), 525.39 (100), 325.19 (12).

In the ^{1}H NMR spectra of **3a**/**3b**, δ 0.80–2.10 ppm (characteristic profile of the substrate). H-3 appears as a double–doublet at δ = 4.69 ppm and H-12 as a triplet at δ = 5.14 ppm of the α-amyrin derivative and δ = 5.20 ppm of the β-amyrin derivative. H-1′ appear as a doublet at δ = 6.39 ppm with ^3J = 12.8 Hz and H-2′ as a doublet at δ = 6.46 ppm with ^3J = 12.8 Hz, which agrees with a *trans*-configuration. In the ^{13}C NMR, the signal for C-3 is at δ = δ = 85.3 ppm, while C-12 appears at δ = 124.3 ppm of the α-amyrin derivative and δ = 121.7 ppm of the β-amyrin derivative, C-13 at δ = 139.9 ppm of the α-amyrin derivative and δ = 145.5 ppm of the β-amyrin derivative. The signal for C-1′ is at δ = 136.9 ppm and for C-2′ at δ = 129.9 ppm. The C=O carbon atoms appear at δ = 164.6 ppm for esters and δ = 167.9 for acids. MS (70 eV) *m*/*z* (%) 524 (37, M^+), 523.37 (100).

The IR spectra of **4a**/**4b** showed the expected absorption band for (C=O) of esters at 1727 cm^{-1}, and also showed an absorption band at 3461 cm^{-1} corresponding to (OH) of acids. In the ^{1}H NMR spectra of **4a**/**4b**, δ 0.80–2.10 ppm (characteristic profile of the substrate). H-3 appears as a double–doublet at δ = 4.52 ppm and H-12 as a triplet at δ = 5.13 ppm of the α-amyrin derivative and δ = 5.21 ppm of the β-amyrin derivative. The signals of H-1′ and H-3′ appear as a double–triplet at δ = 2.44 and 2.41 ppm with ^3J = 7.40 Hz and 7.45 Hz respective and H-2′ as multiplet at δ = 1.98 ppm. In the ^{13}C NMR, the signal for C-3 is at δ = 81.4 ppm, while C-12 appears at δ = 124.5 of the α-amyrin derivative and δ = 121.8 ppm of the β-amyrin derivative, C-13 at δ = 139.8 ppm of the α-amyrin derivative and δ = 145.4 ppm de β-amyrin derivative. Signals for C-1′, C-2′ and C-3′ are at δ = 33.2, 20.2 and 33.87 ppm, respectively. The C=O carbon atoms appear at δ = 172.9 ppm for esters and δ = 178.7 ppm for acids. MS (70 eV) *m*/*z* (%) 540.41 (37, M^+), 539.41 (100), 339.19 (12). Analysis of DEPT - 135° nd 2D-heteronuclear NMR spectra (HSQC and HMBC) provided the final structural elucidation of compounds **1a**/**1b**, **2a**/**2b**, **3a**/**3b** and **4a**/**4b**.

2.2. Cytotoxic activity of α,β-amyrin derivatives

The cytotoxic activity of α,β-amyrin derivatives was determined by the MTT assay using four human tumor cell lines (HL-60, MDAMB-435, SF-295 and HCT-8). The results after 72 h of incubation (Table 1) show that only the derivatives **3a**/**3b** were cytotoxic against the cell lines used. The derivatives **3a**/**3b** showed IC_{50} values ranging from 0.94 (1.8 μM) to 1.84 μg/mL (3.0 μM). From a structure–activity point of view, the high cytotoxicity of **3a**/**3b** can be attributed to the presence of the double bond in the maleinate group attached to carbon 3 of the A ring, which is absent in the other derivatives lacking cytotoxicity. Chemically, the presence of the double bond between carbons C-1′ and C-2′ in the acyl group of the derivatives **3a**/**3b** generates an electron-rich center likely to interact with centers of low electron density. Furthermore, this double bond is in a conjugated system susceptible to resonance that can create positive and negative centers partially able to promote chemical interactions with centers rich or deficient in electrons, which is not observed in the acyl groups of other derivatives (without activity). In fact, many studies have shown a

Table 1
Cytotoxic effect of derivatives of α- and β-amyrin on human tumor cell lines and peripheral blood mononuclear cells

Compound	IC_{50} μg/mL[a] (μM)				
	HL-60	MDAMB-435	SF-295	HCT-8	PBMC
1a/**1b**	>5 (8.5)	>5	>5	>5	>5
2a/**2b**	>5 (9.2)	>5	>5	>5	>5
3a/**3b**	0.94 (1.8) 0.72–1.22	1.52 (2.9) 1.33–1.73	1.84 (3.5) 1.53–2.21	1.58 (3.0) 1.33–1.88	>5 (9.5)
4a/**4b**	>5 (9.2)	>5	>5	>5	>5
Dox[b]	0.02 (0.03) 0.01–0.02	0.48 (0.8) 0.34–0.66	0.24 (0.4) 0.17–0.36	0.01 (0.02) 0.01–0.02	0.97 (1.7) 0.52–1.80

[a] Concentration able to inhibit 50% of cell growth.
[b] Positive control, doxorubicin.

positive relationship between the presence of double bond (unsaturation) in the structure of the compound and the potential cytotoxic effect.[20,21] Cavalcanti et al. demonstrated the importance of the exocyclic double bond in karen-19-oic acid in the induction of DNA damage and subsequent apoptosis of HL-60 cells. Also in this work, karen-19-oic acid was able to interact with cellular DNA and interfere with the catalytic activity of the enzyme topoisomerase I.[22] Alternatively, the presence of the double bond between carbons C-1′ and C-2′ in the derivatives **3a**/**3b** may be related to ROS production. Its oxidation leads to the production of lipid hydroperoxides and non-radical intermediates. These by-products can interact with DNA and altered gene expression, resulting in cell death.[23]

These results confirm that small changes in the molecule can significantly alter the biological effect of a compound, being valid, thus, the production of derived by chemical techniques for semi-synthesis in the search for new drugs, including anticancer.[18] Cragg et al. have been reported that compounds from natural sources have high anticancer potential, they need to be optimized for removal, modification, introduction of functional groups and stereocenters to improve its properties.[24] Combinatorial biosynthetic methods are limited, however, there are numerous examples including the taxanes, camptothecins and combretastatins.[25–27]

Interestingly, in the Alamar Blue assay using human peripheral blood mononuclear cells (PBMC, normal cells), the derivatives **3a**/**3b** were not cytotoxic at the concentrations tested (>5 μg/mL), suggesting selectivity for tumor cells. Additionally, none of the derivatives tested showed hemolytic activity (>50 μg/mL) using mouse erythrocytes, which makes us suspect the activation of a more specific cell death which does not involve the immediate lysis of the cell membrane.

The cytotoxicity results for the derivatives **3a**/**3b** are interesting because the prototype molecule is devoid of anticancer effect, but has instead gastroprotective and antioxidant properties.[11] Therefore, the following experiments were carried out aimed at understanding the mechanism of action of the cytotoxic derivatives **3a**/**3b** in the HL-60 cell line.

2.3. Morphological changes typical of apoptosis induced by 3a/3b

All experiments to investigate the mechanism of action of derivatives **3a**/**3b** in HL-60 cells were accompanied by the trypan blue test to verify cell viability and ensure that the compounds tested maintained their activity. As seen in Figure 2 **3a**/**3b** reduced the number of viable cells and increased the number of non-viable cells in a concentration-dependent manner.

Light microscopy was used to verify the morphology of HL-60 cells untreated or treated with **3a**/**3b** and stained with May Grünwald–Giemsa. After 24 h incubation, cells from the negative control exhibited typical non-adherent and round morphology with vacuolization (Fig. 3A). Chromatin condensation and nuclear and cellular fragmentation were observed in the presence of 0.5 μM doxorubicin (Fig. 3B), characteristic of apoptosis. The cells treated with **3a**/**3b** at a concentration of 1.5 μM showed no striking morphological changes (Fig. 3C). On the other hand, at 3 and 6 μM, **3a**/**3b** induced changes typical of apoptosis, including reduction in cell volume, pyknotic nuclei and chromatolysis,[23] which was more intense at the higher concentration. Moreover, there was an increase in the number of small cells with an intact cell membrane (Fig. 3D and E).

To confirm the light microscopy findings, we performed a morphological analysis of cells treated with **3a**/**3b** by staining with AO/EB and examining cells by fluorescence microscopy. The percentages of viable, apoptotic and necrotic cells were calculated. After 24 h, HL-60 cells treated with **3a**/**3b** showed a reduction in cell viability only at concentrations of 3 and 6 μM. At these concentrations, the number of apoptotic cells significantly increased, corroborating the results described above (Fig. 4). The compounds **3a**/**3b** reduced the number of viable cells by 46.61% and 96.17% at concentrations of 3 and 6 μM, respectively. In parallel, the percentage of apoptotic cells at 3 and 6 μM was 35.59% and 71.84%, respectively. With respect to necrosis, a slight increase in number was observed at a concentration of 6 μM (16.22%).

In flow cytometry, treatment of HL-60 cells for 24 h with **3a**/**3b** showed a reduction in cell size and granularity in a concentration-dependent manner. This may be seen in Figure 5 and corroborated by the reduced number of cells with viable normal morphology (note the panel A gates and panel B). Additionally, membrane integrity was essentially preserved (Fig. 5, panel C), supporting the results indicative of cell death by apoptosis. At a concentration of 6 μM, **3a**/**3b** caused disruption of membrane integrity, which may be indicative of cells in the final process of death or secondary necrosis as observed in microscopic analysis.[28] Similarly, 0.5 μM doxorubicin caused a reduction in cell viability and increased number of apoptotic cells.

2.4. DNA fragmentation, phosphatidylserine (PS) externalization and activation of caspases 3/7 induced by 3a/3b

Morphological analysis of HL-60 cells indicated that the probable process of cell death induced by **3a**/**3b** occurs by induction of apoptosis. We therefore proceeded with the determination of DNA fragmentation, cell cycle changes, PS externalization and the activity of the effector caspases 3/7 by flow cytometry, which are also considered marker events of apoptosis.[28,29] After 24 h, DNA fragmentation of HL-60 cells was significantly increased by compounds **3a**/**3b** in a concentration-dependent manner (Table 2). The positive control, doxorubicin (0.5 μM), induced 77.67% (p <0.0001) DNA fragmentation, comparable to the data for the compounds **3a**/**3b** at 3 and 6 μM (61.54% and 84.24%, respectively). Regarding cell cycle analysis, **3a**/**3b** caused the accumulation of cells in G0/G1 phase at 3 μM (30.52%) (p <0.05) and in S phase at 6 μM (88.63%) (p <0.001). Cell cycle arrest could be related to an attempt by the cell to repair the DNA damage caused by **3a**/**3b**. Since the damage appears to be very intense, repair does not occur and apoptosis is triggered.[28]

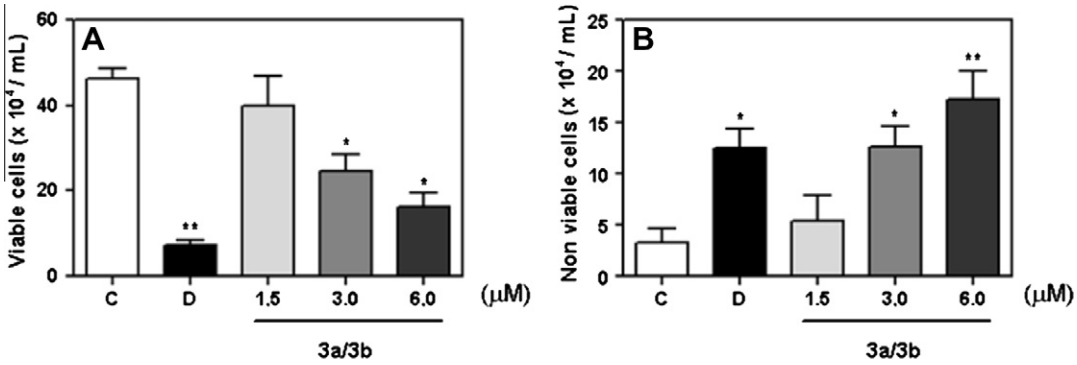

Figure 2. Effect of **3a**/**3b** on HL-60 cell viability determined by trypan blue exclusion after 24 h of incubation. Negative control (C) was treated with the vehicle used for diluting the test compound. Doxorubicin (0.5 μM) was used as the positive control (D). (A) Number of viable cells. (B) Number of non viable cells. Results are expressed as mean ± standard error of mean (SEM) for multiple independent experiments. $^{*}p$ <0.05; $^{**}p$ <0.001 compared to control by ANOVA followed by Dunnett's test.

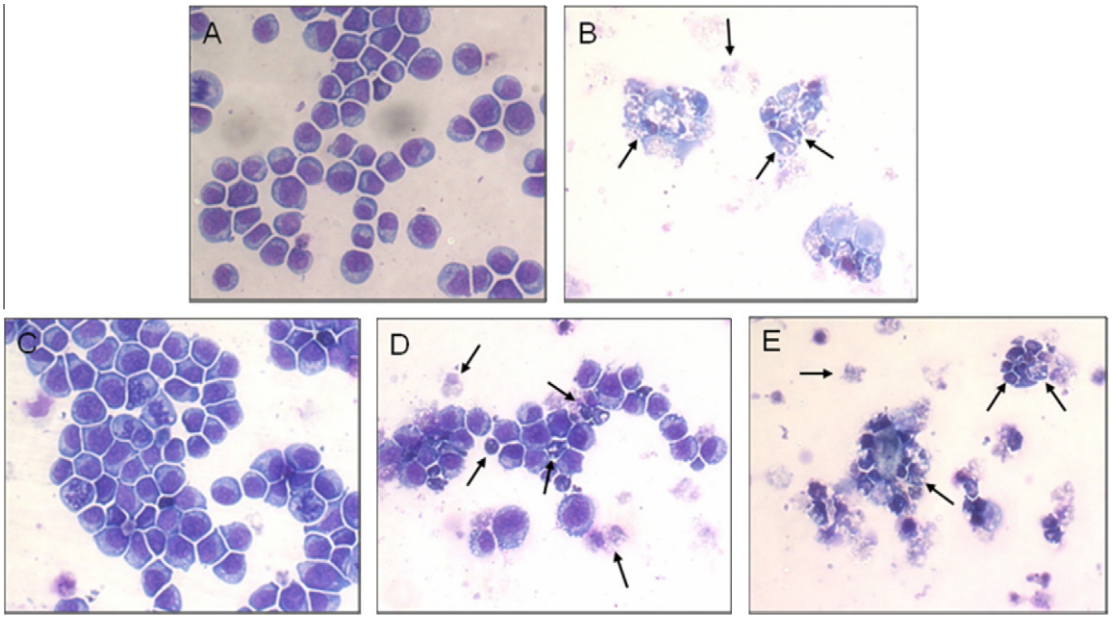

Figure 3. Microscopic analysis (May Grünwald/Giemsa-stained) of effect of **3a**/**3b** on HL-60 cell after 24 h of incubation. Cells untreated (A) or treated with **3a**/**3b** (1.5 μM, C; 3 μM, D; or 6 μM, E) were analyzed by light microscopy (200×). Doxorubicin (0.5 μM) was used as the positive control (B). Black arrows show reduction of cell volume, nuclear fragmentation and cellular debris.

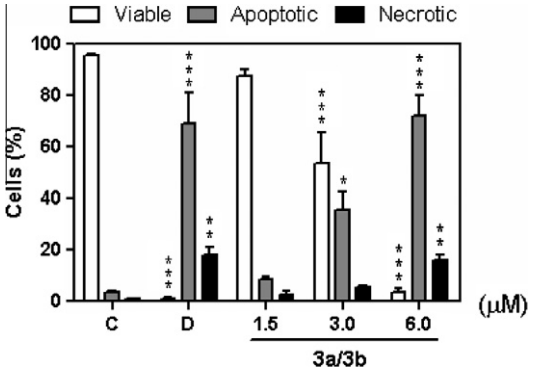

Figure 4. Effect of **3a**/**3b** on HL-60 cell death pattern determined by acridine orange and ethidium bromide-staining (AO/EB) after 24 h of incubation. Negative control (C) was treated with the vehicle used for diluting the test compound. Doxorubicin (0.5 μM) was used as the positive control (D). Results are expressed as mean ± standard error of mean (SEM) for three independent experiments performed in duplicate (n = 6). $^{*}p$ <0.05; $^{**}p$ <0.001; $^{***}p$ <0.0001 compared to control by ANOVA followed by Dunnett's test.

The detection of PS externalization showed that **3a**/**3b** significantly induced apoptosis (Fig. 6A), especially at 6 μM (44.22%) (p <0.0001). In parallel, it was found that **3a**/**3b** was also able to activate caspases 3/7 in a significant and concentration-dependent manner. The results showed that 7.88% and 21.58% of cells had activated caspases 3/7 at 3 and 6 μM, respectively (Fig. 6B). All results presented herein suggest that compounds **3a**/**3b** induce cell death by apoptosis in HL-60 leukemia cells.

3. Conclusions

Despite all the technological advances, the treatment of cancer is still a challenge and cases of cure are rare. Natural products and chemical modification of antitumor substances are among the most important strategies used in the search of new antineoplastic drugs.[30] Therefore, the objective of this study was to extract and identify the triterpenoid mixture of α- and β-amyrin, as well as, to produce new derivatives and determine their cytotoxic effects on human tumor cell lines and normal cells.

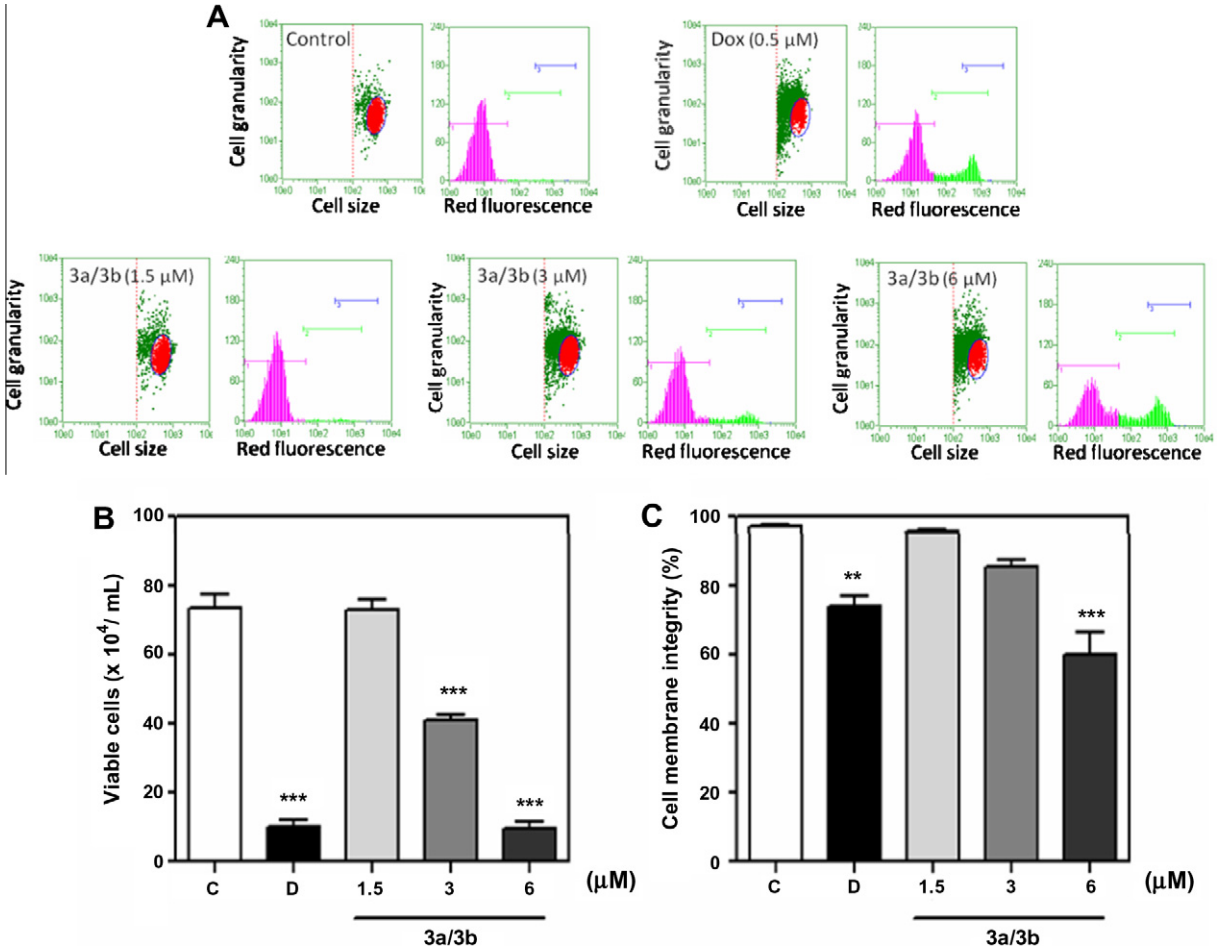

Figure 5. Effects of **3a**/**3b** (1.5, 3 and 6 μM) on HL-60 cell population determined by flow cytometry using propidium iodide, after 24 h of incubation. The negative control (**C**) was treated with the vehicle used for diluting the test compound. Doxorubicin (0.5 μM) was used as the positive control (D). (**Panel A**) The forward light scatter and side light scatter of the laser were used as indices of cell size and granularity, respectively. (**Panel B**) Number of viable cells by size and granularity (gated cells in panel A). (**Panel C**) Percentage of cells with intact membrane. Results are expressed as mean ± standard error of mean (SEM) for three independent experiments performed in duplicate ($n = 6$). $^{**}p$ <0.001; $^{***}p$ <0.0001 compared to control by ANOVA followed by Dunnett's test.

Table 2
Effect of **3a**/**3b** on the nuclear DNA content of HL-60 cells determined by flow cytometry after 24 h of incubation

Compound	Concentration (μM)	DNA[b] (%)			
		Sub-G0/G_1	G0/G_1	S	G_2/M
Control	–	8.25 ± 0.15	22.07 ± 0.43	67.13 ± 1.09	11.83 ± 1.08
Doxorubicin[a]	0.5	77.67 ± 2.41***	19.67 ± 3.72	78.91 ± 4.84	1.41 ± 1.11***
3a/**3b**	1.5	17.57 ± 1.17**	25.17 ± 2.92	67.41 ± 3.27	7.41 ± 0.62*
	3.0	61. 54 ± 0.52***	30.52 ± 2.66**	64.92 ± 1.95	4.57 ± 1.29**
	6.0	84.24 ± 1.16***	7.11 ± 0.56**	88.63 ± 3.65**	0.04 ± 0.04***

$^{*}p$ <0.05; $^{**}p$ <0.001; $^{***}p$ <0.0001, compared to control by ANOVA followed by Dunnett's test.
[a] Doxorubicin (0.5 μM) was used as the positive control.
[b] Results are expressed as mean ± standard error of mean (SEM) for three independent experiments performed in duplicate ($n = 6$).

In this study, we demonstrated that among the mixtures of derivatives of α,β-amyrin tested, the mixture **3a**/**3b** stood out because of its high cytotoxic effect on human tumor cell lines, with highest activity in HL-60 cells. This activity is possibly related to the presence of the maleinate group linked to C-3 of the A ring of the triterpenoid skeleton. There is a positive correlation between the IC_{50} and the presence of the double bond in this group, due the possibility to interact with cellular DNA, inhibiting the enzyme topoisomerase I, or lipid peroxidation generates a large amount of by-products and adduct formation, which can damage the DNA and altered gene expression.[22,23] Additionally, **3a**/**3b** seemed to be selective for tumor cells, since they were not toxic to normal PBMC cells. Regarding the mechanism of action, **3a**/**3b** induced the death of HL-60 cells by the induction of apoptosis, which was demonstrated by morphological analysis (volume reduction, maintenance of cell membrane integrity and nuclear fragmentation), DNA fragmentation, externalization of PS and activation of caspases 3/7.[29,31,32]

The esterases could be a critical point in this work, but another researches concluded that some of the non-natural ester analogues

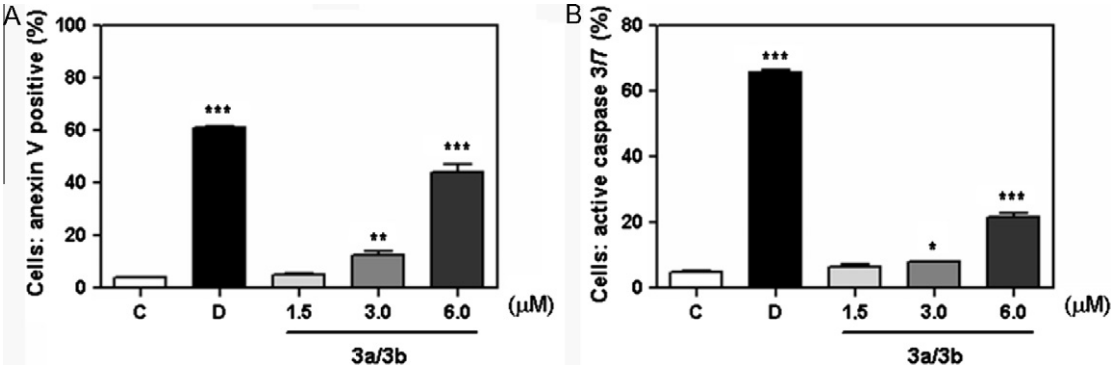

Figure 6. Effect of **3a**/**3b** on PS externalization (**Panel A**) and caspase 3/7 activation (**Panel B**) of HL-60 cells by flow cytometry after 24 h of incubation. Negative control (C) was treated with the vehicle used for diluting the test compound. Doxorubicin (0.5 μM) was used as the positive control (D). Results are expressed as mean ± standard error of mean (SEM) for two independent experiments performed in triplicate ($n = 6$). $^{*}p$ <0.05; $^{**}p$ <0.001; $^{***}p$ <0.0001, compared to control by ANOVA followed by Dunnett's test.

of the naturally occurring α-amyrin are better glucose ameliorating than the naturally isolated α-amyrin acetate and almost as equipotent as metformin.[33] The by-products in this organic reaction could be more effective than the original compound. To measure this reaction in vivo will be the next step in this work. Nanoscience and nanotechnology strategies for imaging and treating cancer could be useful to design a method to avoid the esterases action, like another works that find a combinatorial drug delivery nanocapsule with sequential delivery feature for effective antivasculature and anticancer activities in vitro and in vivo.[34] Among the various approaches considered, nanotechnology offers the best promise for the targeted delivery of drugs and genes to a tumor site and for alleviating side effects of chemotherapeutic agents. Renowned industrial and academic researchers describe the advantages of nanoparticles as sensing, delivery, image enhancement agents for cancer treatments, and various types of useful nanoparticles such as polymeric nanoparticles and dendrimers.[35,36]

4. Experimental

4.1. Chemistry

The melting point was determined using a Mettler Toledo FP82HT micromelting point apparatus. The IR spectra were measured in KBr pellets using a Perkin-Elmer FT-IR Spectrum 1000. All NMR data were recorded using a Bruker Avance DPX 300 and Avance DRX-500 spectrometer operating at the frequency of the hydrogen at 300.13 and 500.13 MHz in the frequency of the carbon for 75.47 and 125.75 MHz, using $CDCl_3$ as the solvent. High resolution data were obtained in a MS-IT-TOF mass spectrometer.

4.1.1. Procedure for the synthesis of the derivatives of α,β-amyrin

4.1.1.1. 3-*O*-Carboxybenzoate of α,β-amyrin (1a/1b). The mixture of α,β-amyrin (**a**/**b**), 100 mg, was dissolved in 20 mL of ethyl ether and added to a solution of phthalic anhydride (139 mg in 20 mL of ethyl ether) in pyridine (0.5 mL); the reaction proceeded under reflux for 8 h at a temperature of 50 °C. The final solution was added to 15 mL of a concentrated solution of copper sulfate, and the organic phase was separated and evaporated to dryness at room temperature. The reaction material was chromatographed on a silica gel column eluted with EtOAc, yielding 58.4 mg (43%).

4.1.1.2. 3-*O*-Carboxysuccinate of α,β-amyrin (2a/2b). The mixture of α,β-amyrin (**a**/**b**), 100 mg, was dissolved in 20 mL of CH_2Cl_2 and then added a solution of succinic anhydride (43.67 mg in 20 mL of CH_2Cl_2) and DMAP in catalytic amounts, with subsequent refluxing for 8 h at a temperature of 50 °C. The solution was concentrated and the resulting solid was chromatographed on a silica gel column eluted with EtOAc, yielding 45.84 mg (37%).

4.1.1.3. 3-*O*-Carboxymaleinate of α,β-amyrin (3a/3b). The mixture of α,β-amyrin (**a**/**b**), 200 mg, was dissolved in 20 mL of CH_2Cl_2 and then added to a solution of maleic anhydride (184 mg in 20 mL of CH_2Cl_2). The mixture was then refluxed for 8 h at a temperature of 50 °C. The solution was concentrated under vacuum and the resulting solid chromatographed on a silica gel column eluted with EtOAc, yielding 76.27 mg (31%).

4.1.1.4. 3-*O*-Carboxyglutarate of α,β-amyrin (4a/4b). The mixture of α,β-amyrin (**a**/**b**), 100 mg, was dissolved in 20 mL of CH_2Cl_2 and then added to a solution of glutaric anhydride (26.76 mg in 20 mL of CH_2Cl_2) and DMAP in catalytic amounts, with subsequent refluxing for 8 h at a temperature of 50 °C. The reaction product was concentrated under vacuum and the resulting solid chromatographed on a silica gel column eluted with EtOAc, yielding 92 mg (35%).

4.1.2. 3-*O*-Carboxybenzoate of α,β-amyrin (1a/1b)

White solid, 43% yield; mp: 135 °C. FTIR (KBr) ν (cm^{-1}): 3461, 2925, 1701, 1583, 1404. ^{1}H NMR (500 MHz, $CDCl_3$) δ 4.77 (dd, H-3), 5.13 (t, H-12 of the α-amyrin derivative), 5.19 (t, H-12 of the β-amyrin derivative). ^{13}C (125 MHz, $CDCl_3$) δ 38.7/38.2 (C-1), 26.8 (C-2), 83.3 (C-3), 38.2 (C-4), 55, 6 (C-5), 18.4 (C-6), 33.1/33.5 (C-7), 40.0/39.8 (C-8), 47.9/47.8 (C-9), 38.0 (C-10), 23.5/23.6 (C-11), 124.5/121.9 (C-12), 139.8/145.4 (C-13), 41.8/40.0 (C-14), 28.3/26.8 (C-15), 26.8 (C-16), 33.6/33.1 (C-17), 59.3/47.5 (C-18), 39.8/47.5 (C-19), 39.2/31.5 (C-20), 31.5/33.7 (C- 21), 41.8/38.0 (C-22), 28.3/28.4 (C-23), 15.9 (C-24), 15.9 (C-25), 17.1/17.0 (C-26), 23.1/26.8 (C-27), 28.9/28.4 (C-28), 17.8/33.6 (C-29), 21. 6 (C-30), 168.1/172.1 (C═O), 131.9 (C-1′), 129.1 (C-2′), 133.4 (C-3′), 131.1 (C-4′), 130.1 (C-5′), 131.1 (C-6′).

4.1.3. 3-*O*-Carboxysuccinate of α,β-amyrin (2a/2b)

White solid, 37% yield; mp: 200 °C. FTIR (KBr) ν (cm^{-1}): 3446, 2925, 1731, 1715, 1450. ^{1}H NMR (500 MHz, $CDCl_3$) δ 4.54 (dd, H-3), 5.13 (t, H-12 of the α-amyrin derivative), 5.21 (t, H-12 of the β-amyrin derivative), 2.64 (dd, J = 5.40 and 5.85 Hz, H-1′), 2.69 (dd, J = 5.40 and 5.85 Hz, H-2′). ^{13}C (125 MHz, $CDCl_3$) δ 38.7/38.0 (C-1), 26.8 (C-2), 81.8 (C-3), 38.0 (C-4), 55, 5 (C-5), 18.4 (C-6), 31.7 (C-7), 39.9 (C-8), 47.8/47.6 (C-9), 37.9 (C-10), 23.1/23.7 (C-11), 124.5/121.8 (C-12), 139.9/145.4 (C-13), 41.8/40.0 (C-14), 28.2/26.8 (C-15), 26.8 (C-16), 33.1/31.5 (C-17), 59.3/ 47.5

(C-18), 39.8/47.8 (C-19), 39.5/31.0 (C-20), 31.5/33.1 (C-21), 41.6/38.0 (C-22), 28.2/28.3 (C-23), 16.0/15.9 (C-24), 15.9 (C-25), 16.9/16.0 (C-26), 23.5/26.0 (C-27), 28.3/28.2 (C-28), 17.7/33.5 (C-29), 21.6 (C-30), 172.9/178.7 (C=O), 28.2 (C-1′), 28.2 (C-2′).

4.1.4. 3-*O*-Carboxymaleinate of α,β-amyrin (3a/3b)

White solid, 31% yield; mp: 188 °C FTIR (KBr) ν (cm^{-1}): 3422, 2924, 1722, 1633, 1454. ^{1}H NMR (500 MHz, $CDCl_3$) δ 4.69 (dd, H-3), 5.14 (t, H-12 of the α-amyrin derivative), 5.20 (t, H-12 of the β-amyrin derivative), 6.39 (d, J = 12.8 Hz, H-1′), 6.47 (d, J = 12.8 H, H-2′). ^{13}C (125 MHz, $CDCl_3$) δ C 38.6/38.4 (C-1), 27.1 (C-2), 85.3 (C-3), 37.3 (C-4), 55.5 (C-5), 18.4 (C-6), 32.7 (C-7), 40.2/40.0 (C-8), 47.9/47.8 (C-9), 37.0 (C-10), 23.6/23.7 (C-11), 124.3/121.7 (C-12), 139.9/145.3 (C-13), 42.3/41.9 (C-14), 28.3/26.3 (C-15), 26.8 (C-16), 33.9/32.7 (C-17), 59.3/47.4 (C-18), 39.8/47.0 (C-19), 39.8/31.0 (C-20), 31.4/35.0 (C-21), 41.7/37.3 (C-22), 28.3 (C-23), 15.9/13.7 (C-24), 15.9/15.7 (C-25), 16.9/16.8 (C-26), 23.5/26.2 (C-27), 28.6/28.3 (C-28), 17.7/33.5 (C-29), 21.6 (C-30), 164.6/167.9 (C=O), 136.9 (C-1′), 129.9 (C-2′).

4.1.5. 3-*O*-Carboxyglutarate of α,β-amyrin (4a/4b)

White solid, 35% yield; mp: 209 °C. FTIR (KBr) ν (cm^{-1}): 3461, 2924, 1727, 1455. ^{1}H NMR (500 MHz, $CDCl_3$) δ 4.52 (dd, H-3), 5.13 (t, H-12 of the α-amyrin derivative), 5.21 (t, H-12 of the β-amyrin derivative), 2.40 (t, J = 7.3 Hz, H-1′), 2.44 (t, J = 7.4 Hz, H-3′), 1.98 (m, H-2′). ^{13}C (125 MHz, $CDCl_3$) δ 38.6/38.5 (C-1), 27.1 (C-2), 81.4 (C-3), 37.9 (C-4), 55.5 (C-5), 18.4 (C-6), 32.7 (C-7), 40.2/40.0 (C-8), 47.8/47.7 (C-9), 37.1 (C-10), 23.6/23.7 (C-11), 124.5/121.8 (C-12), 139.8/145.4 (C-13), 42.3/41.9 (C-14), 28.3/26.3 (C-15), 26.8 (C-16), 33.9/32.7 (C-17), 59.3/47.4 (C-18), 39.8/47.0 (C-19), 39.9/31.2 (C-20), 31.5/34.9 (C-21), 41.8/37.4 (C-22), 28.3 (C-23), 15.9/15.8 (C-24), 15.9/15.8 (C-25), 17.0/16.9 (C-26), 23.5/26.2 (C-27), 28.6/28.3 (C-28), 17.7/33.5 (C-29), 21.6 (C-30), 172.9/178.7 (C=O), 33.2 (C-1′), 20.2 (C-2′), 33.8 (C-3′).

4.2. Biology

4.2.1. Cytotoxicity against cancer cell lines—MTT assay

The cytotoxic effect of compounds was evaluated by the MTT assay,[37] using four human cancer cell lines: HL-60 (promyelocytic leukemia), SF-295 (glioblastoma), HCT-8 (colon cancer) and MDAMB-435 (melanoma), all obtained from the National Cancer Institute (Bethesda, MD, USA). All cell lines were maintained in RPMI 1640 medium supplemented with 10% fetal bovine serum, 2 mM glutamine, 100 U/mL penicillin and 100 μg/mL streptomycin, at 37 °C with 5% CO_2. Cancer cell growth was quantified by the ability of living cells to reduce the yellow dye 3-(4,5-dimethyl-2-thiazolyl)-2,5-diphenyl-2*H*-tetrazolium bromide (MTT) (Sigma Aldrich Co., St. Louis, MO/USA) to a purple formazan product. Briefly, cells were seeded in 96-well plates (0.7×10^5 cells/well for adherent cells and 0.3×10^6 cells/well for suspended cells), and compounds (0.078–5 μg/mL) dissolved in DMSO were added to each plate well. Control groups received the same amount of vehicle. The final concentration of DMSO in the culture medium was kept constant, below 0.1% (v/v). After 72 h of incubation, the supernatant was replaced by fresh medium containing MTT (0.5 mg/mL). Three hours later, the MTT formazan product was dissolved in 150 μL DMSO, and absorbance was measured at 595 nm (DTX-880 Multimode Detector, Beckman Coulter®). All cell treatments were carried out in triplicate and doxorubicin was used as the positive control.

4.2.2. Inhibition of PBMC proliferation—Alamar Blue assay

In order to investigate the effect of the test compounds on normal proliferating cells, the Alamar Blue assay[38] was performed with human peripheral blood mononuclear cells (PBMC) after 72 h drug exposure. Heparinized blood (from healthy, non-smoker donors who had not taken any drug at least 15 days prior to sampling) was collected and PBMC were isolated by a standard method of density-gradient centrifugation over Ficoll-Hypaque. PBMC were washed and resuspended at a concentration of 3×10^5 cells/mL in RPMI 1640 medium supplemented with 20% fetal bovine serum, 2 mM glutamine, 100 U/mL penicillin and 100 μg/mL streptomycin, at 37 °C with 5% CO_2. Phytohemagglutinin (3%) was added at the beginning of culture. After 24 h, the compounds (0.078–5 μg/mL) dissolved in DMSO were added to each plate well, and the cells were incubated for 72 h. Control groups received the same amount of vehicle and doxorubicin was used as the positive control. The final concentration of DMSO in the culture medium was kept constant, below 0.1% (v/v). Twenty-four hours before the end of the incubation, 10 μL of stock solution (0.312 mg/mL) of the Alamar Blue (Resazurin, Sigma–Aldrich Co) was added to each well. The absorbance was measured using a multiplate reader (DTX 880 Multimode Detector, Beckman Coulter®) and the drug effect was expressed as the percentage of control absorbance at 570 nm and 595 nm.

4.2.3. Hemolytic assay

The test was performed in 96-well plates using a 2% mouse erythrocyte suspension in 0.85% NaCl containing 10 mM $CaCl_2$, following the method described by Jimenez et al.[39] The compounds were tested at concentrations ranging from 0.38 to 200 μg/mL. After incubation (1 h) at room temperature, the supernatant was removed and the hemoglobin released was measured spectrophotometrically at 540 nm. DMSO at 10% was used as the negative control and Triton X-100 (1%) was used as the positive control.

4.2.4. Study of the mechanism of cytotoxicity induced by 3-*O*-carboximaleinate of α- and β-amyrin (3a/3b)

In the second stage of the study aimed at determining the cytotoxicity induced by **3a**/**3b**, the HL-60 promyelocytic leukemia cell line was chosen based on preliminary cytotoxicity screening (MTT assay).

The HL-60 cell line is one of the most often used model for studying cytotoxic substances.[40,41] Therefore, the following experiments were performed using HL-60 cells as a model and **3a**/**3b** were dissolved in sterile DMSO (vehicle control). The cells were incubated with the test compounds for 24 h at three different concentrations (1.5, 3.0 and 6.0 μM), chosen based on IC_{50} values obtained by the MTT assay. Doxorubicin (0.5 μM) was used as the positive control.

4.2.4.1. Cell viability by trypan blue exclusion. Cell viability was determined by the trypan blue dye exclusion test[42] after treatment. Cells (0.3×10^6 cells/mL) were incubated with **3a**/**3b**, and trypan blue-excluding cells were counted in a Neubauer chamber, using an aliquot of cells removed from cultures after incubation.

4.2.4.2. Analysis of morphological changes. Untreated and treated HL-60 cells were examined for morphological changes by light microscopy (Olympus, Tokyo, Japan). Cells from cultures after 24 h were harvested, transferred to cytospin slides, fixed with methanol for 1 min and stained with May Grünwald–Giemsa (Bioclin, Brazil).

4.2.4.3. Morphological analysis with fluorescence microscopy. Acridine orange/ethidium bromide (AO/EB) (Sigma Aldrich) staining[43] of HL-60 cells was performed to evaluate the cell death pattern induced by increasing concentrations of compounds. After incubation, cells were pelleted and each sample was mixed with 1 μL of aqueous AO/EB solution (100 μg/mL of AO in PBS; 100 μg/mL EB in PBS) just prior to fluorescence microscopy and quantification (Olympus, Tokyo, Japan). Three hundred cells were counted per sample and scored as follows: viable cells,

apoptotic cells and necrotic cells.[44,45] The percentage of apoptotic and necrotic cells was calculated.

4.2.4.4. Flow cytometry analysis. HL-60 cell fluorescence was determined by flow cytometry in a Guava EasyCyte Mine using Guava Express Plus software. Five thousand events were analyzed for each replicate in three independent experiments, and cellular debris was omitted from the analysis. Internucleosomal DNA fragmentation and cell cycle were determined by ModFit LT for Win32 version 3.1.

4.2.5. Cell membrane integrity

The cell membrane integrity was evaluated by the exclusion of propidium iodide (50 μg/mL, Sigma Aldrich Co., St. Louis, MO/USA). Briefly, a 100 μL suspension of treated and untreated cells was incubated with propidium iodide (50 μg/mL). The cells were then incubated for 5 min. Fluorescence was measured and analyzed for cell morphology, granularity and membrane integrity.[46]

4.2.6. Internucleosomal DNA fragmentation and cell cycle analysis

DNA fragmentation and cell cycle were analyzed by flow cytometry after DNA staining with propidium iodide. Briefly, a 100 μL suspension of treated and untreated cells was incubated for 30 min, in the dark, with hypotonic solution containing 50 μg/mL propidium iodide, 0.1% sodium citrate, and 0.1% Triton X-100. Fluorescence was measured and DNA fragmentation and cell cycle phases were determined.[47]

4.2.7. Phosphatidylserine (PS) externalization

PS externalization was analyzed by flow cytometry after PS staining with Annexin V according to the method described by Vermes et al.[48] The Guava Nexin Assay Kit was used to determine early apoptosis. Cells were washed twice with cold PBS and then resuspended in 135 μL of PBS with 5 μL of 7-amino-actinomycin D (7AAD) and 10 μL of Annexin V-PE. The cells were gently vortexed and incubated for 20 min at room temperature (20–25 °C) in the dark. Afterward, the cells were analyzed by flow cytometry (EasyCyte from Guava Technologies). Annexin V is a phospholipid-binding protein that has a high affinity for PS. 7-AAD, a cell impermeant dye, is used as an indicator of membrane structural integrity. Annexin V-PE was measured as a yellow fluorescence at 583 nm and 7-AAD as a red fluorescence at 680 nm. The percentage of early and late apoptotic cells and necrotic cells was then calculated.

4.2.8. Activity of caspases 3 and 7

Caspase 3/7 activity was analyzed by flow cytometry, using Guava® EasyCyte Caspase Kit, after 24 h of incubation. HL-60 cells (3×10^5 cells/mL) were incubated with Fluorescent Labeled Inhibitor of Caspases (FLICA) and maintained for 1 h at 37 °C and 5% CO_2. After incubation, 80 μL of washing buffer were added and cells were centrifuged at 2000 rpm for 5 min. The resulting pellet was resuspended in 200 μL of washing buffer and centrifuged again. The cells were then resuspended in the working solution (propidium iodide 1:200 in 1× washing buffer) and analyzed immediately using flow cytometry.

4.3. Statistical analysis

For cytotoxicity assays, the IC_{50} or EC_{50} values and their 95% confidence intervals were obtained by nonlinear regression using the GraphPad program (Intuitive Software for Science, San Diego, CA). Data obtained from the studies of mechanism of action are presented as means ± SEM for at least three independent experiments and evaluated by ANOVA followed by the Student Newman–Keuls test.

5. Conflict of interest statement

None

Acknowledgments

This research received financial support from FUNCAP, CNPq and CAPES. The authors thank National Cancer Institute (Bethesda, MD, USA) for donating the tumor cell lines used in this study and CENAUREM for conducting the NMR spectra. Dr. A. Leyva provided English editing of the manuscript.

References and notes

1. Mahato, S. B.; Nandy, A. K.; Roy, G. *Phytochemistry* **1992**, *31*, 2199.
2. Mahato, S. B.; Sen, S. *Phytochemistry* **1997**, *44*, 1185.
3. Oliveira, F. A.; Costa, C. L. S.; Chaves, M. H.; Almeida, F. R. C.; Cavalcante, I. J. M.; Lima, A. F.; Lima, R. C. P., Jr.; Silva, R. M.; Campos, A. R.; Santos, F. A.; Rao, V. S. N. *Life Sci.* **2005**, *77*, 2942.
4. Keterere, D. R.; Gray, A. I.; Nash, R. J.; Waigh, R. D. *Phytochemistry* **2003**, *63*, 81.
5. Oliveira, F. A.; Lima, R. C. P., Jr.; Cordeiro, W. M.; Vieira, G. M., Jr.; Chaves, M. H.; Almeida, F. R. C.; Silva, R. M.; Santos, F. A.; Rao, V. S. N. *Pharmacol. Biochem. Behav.* **2004**, *78*, 719.
6. Oliveira, F. A.; Vieira, H. M., Jr.; Chaves, M. H.; Almeida, F. R. C.; Florêncio, M. G.; Lima, R. C. P., Jr.; Silva, R. M.; Santos, F. A.; Rao, V. S. N. *Pharmacol. Res.* **2004**, *49*, 105.
7. Pinto, S. A. H.; Pinto, L. M. S.; Cunha, G. M. A.; Chaves, M. H.; Santos, F. A.; Rao, V. S. N. *Inflammopharmacology* **2008**, *16*, 48.
8. Pinto, S. A. H.; Pinto, L. M. S.; Guedes, G. M. A.; Cunha, G. M. A.; Chaves, M. H.; Santos, F. A.; Rao, V. S. N. *Phytomedicine* **2008**, *15*, 630.
9. Aragão, G. F.; Carneiro, L. M. V.; Junior, A. P. F.; Vieira, L. C.; Bandeira, P. N.; Lemos, T. L. G.; Viana, G. S. B. *Pharmacol. Biochem. Behav.* **2006**, *85*, 827.
10. Aragão, G. F.; Cristhiany, C. P.; Bandeira, P. N.; Lemos, T. L. G.; Viana, G. S. B. *J. Herbal Pharmacother.* **2007**, *7*, 31.
11. Laszczyk, M. N. *Planta Med.* **2009**, *75*, 1549.
12. Bandeira, P. N.; Lemos, T. L. G.; Costa, S. M. O.; Santos, H. S. *Rev. Bras. Farmacogn.* **2007**, *17*, 204.
13. Soldi, C.; Latti, M. G. P.; Luiz, A. P.; Marcon, R.; Meotti, F. C.; Mioto, L. A.; Santos, A. R. S. *Bioorg. Med. Chem.* **2008**, 1.
14. Aragão, G. F.; Carneiro, L. M. V.; Junior, A. P. F.; Bandeira, P. N.; Lemos, T. L. G.; Viana, G. S. B. *Pharm. Biol.* **2007**, *45*, 343.
15. Oliveira, F. A.; Lima, R. C. P., Jr.; Cordeira, W. M.; Vieira, G. M., Jr.; Chaves, M. H.; Almeida, F. R. C.; Silva, R. M.; Santos, F. A.; Rao, V. S. N. *Pharmacol. Biochem. Behav.* **2004**, *78*, 718.
16. Fernandes, J.; Castilho, R. O.; Costa, M. R.; Wagner-Souza, K.; Kaplan, M. A. C.; Gattass, C. R. *Cancer Lett.* **2003**, *190*, 165.
17. Sun, H. X.; Ye, Y. P.; Pan, Y. J. *J. Ethnopharmacol.* **2004**, *90*, 261.
18. Lee, K. H. *J. Nat. Prod.* **2010**, *73*, 500.
19. Bandeira, P. N.; Pessoa, O. D. L.; Trevisan, M. T. S.; Lemos, T. L. G. *Quim. Nova* **2002**, *25*, 1078.
20. Amslinger, S. *ChemMedChem* **2010**, *5*, 351.
21. Roh, E. M.; Jin, Q.; Jin, H. G.; Shin, J. E.; Choi, E. J.; Moon, Y. H.; Woo, E. R. *Arch. Pharmacol. Res.* **2010**, *33*, 1347.
22. Cavalcanti, B. C.; Bezerra, D. P.; Magalhães, H. I.; Moraes, M. O.; Lima, M. A.; Silveira, E. R.; Câmara, C. A.; Rao, V. S.; Pessoa, C.; Costa-Lotufo, L. V. *J. Appl. Toxicol.* **2009**, *7*, 560.
23. Pillon, N. J.; Soulère, L.; Vella, R. E.; Croze, M.; Caré, B. R.; Soula, H. A.; Doutheau, A.; Lagarde, M.; Soulage, C. O. *Chem. Biol. Interact.* **2010**, *188*, 171.
24. Cragg, G. M.; Grothaus, P. G.; Newman, D. J.; Cragg, G. M. *Chem. Rev.* **2009**, *109*, 3012.
25. Coseri, S. *Mini-Rev. Med. Chem.* **2009**, *9*, 560.
26. Kingston, D. G. I. *J. Org. Chem.* **2008**, *73*, 3975.
27. Rahier, N. J.; Thomas, C. J.; Hecht, S. M. In *Anticancer Agents from Natural Products*; Cragg, G. M., Kingston, D. G. I., Newman, D. J., Eds.; CRC Press LLC: Boca Raton, FL, 2005; p 5.
28. Maia, D. P.; Wilke, D. V.; Mafezoli, J.; Júnior, J. N. S.; Moraes, M. O.; Pessoa, C.; Costa-Lotufo, L. V. *Chem. Biol. Interact.* **2009**, *180*, 220.
29. Bezerra, D. P.; Militão, G. C. G.; Castro, F. O.; Pessoa, C.; Moraes, M. O.; Silveira, E. R.; Lima, M. A. S.; Elmiro, F. J. M.; Costa-Lotufo, L. V. *Toxicol. In Vitro* **2007**, *21*, 1.
30. Pinkerton, D. M.; Banwell, M. G.; Garson, M. J.; Kumar, N.; Moraes, M. O.; Cavalcanti, B. C.; Barros, F. W. A.; Pessoa, C. *Chem. Biodiv.* **2010**, *7*, 1311.
31. Esteves-Souza, A.; Lucio, K. A.; Da Cunha, A. S.; Da Cunha Pinto, A.; Da Silva Lima, E. L.; Camara, C. A.; Vargas, M. D.; Gattass, C. R. *Oncol. Rep.* **2008**, *20*, 225.
32. Yedjou, C. G.; Milner, J. N.; Howard, C. B.; Tchounwou, P. B. *Int. J. Environ. Res. Public Health.* **2010**, *7*, 2008.

33. Narender, T.; Khaliq, T.; Singh, A. B.; Joshi, M. D.; Mishra, P.; Chaturvedi, J. P.; Srivastava, A. K.; Maurya, R.; Agarwal, S. C. *Eur. J. Med. Chem.* **2009**, *44*, 1215.
34. Wang, Z.; Ho, P. C. *Biomaterials* **2010**, *31*, 7115.
35. Nassar, T.; Rom, A.; Nyska, A.; Benita, S. *Pharm. Res.* **2008**, *25*, 2019.
36. Nassar, T.; Rom, A.; Nyska, A.; Benita, S. *J. Controlled Release* **2009**, *133*, 77.
37. Mosman, T. *J. Immunol. Methods* **1983**, *65*, 55.
38. Zhi-Jun, Y.; Sriranganathan, N.; Vaught, T.; Arastu, S. K.; Ansar-Ahmed, S. *J. Immunol. Methods* **1997**, *210*, 25.
39. Jimenez, P. C.; Fortier, S. C.; Lotufo, T. M. C.; Pessoa, C.; Moraes, M. E. A.; Moraes, M. O.; Costa-Lotufo, L. V. *J. Exp. Marine Biol. Ecol.* **2003**, *287*, 93.
40. Collins, S. J. *Blood* **1987**, *70*, 1233.
41. Militão, G. C. G.; Dantas, I. N. F.; Pessoa, C.; Falcão, M. J. C.; Silveira, E. R.; Lima, M. A. S.; Curi, R.; Lima, T.; Moraes, M. O.; Costa-Lotufo, L. V. *Life Sci.* **2006**, *78*, 2409.
42. Renzi, D.; Valtolina, M.; Foster, R. *Altern. Lab. Anim.* **1993**, *21*, 89.
43. McGahon, A. J.; Martin, S. M.; Bissonnette, R. P.; Mahboubi, A.; Shi, Y.; Mogil, R. J.; Nishioka, W. K.; Green, D. R. *Methods Cell Biol.* **1995**, *46*, 153.
44. Geng, C. X.; Zeng, Z. C.; Wang, J. Y. *World J. Gastroenterol.* **2003**, *9*, 696.
45. Cury-Boaventura, M. F.; Pompeia, C.; Curi, R. *Clin. Nutr.* **2004**, *23*, 721.
46. Darzynkiewicz, Z.; Bruno, S.; Del Bino, G.; Gorczyca, W.; Hotz, M. A.; Lassota, P.; Traganos, F. *Cytometry* **1992**, *13*, 795.
47. Nicoletti, I.; Migliorati, G.; Pagliacci, M. C.; Grignani, F.; Riccardi, C. *J. Immunol. Methods* **1991**, *139*, 271.
48. Vermes, I.; Haanen, C.; Steffens-Nakken, H.; Reutlingsperger, C. *J. Immunol. Methods* **1995**, *184*, 39.